Materials and Design 31 (2010) 3954–3959

Contents lists available at ScienceDirect

Materials and Design

journal homepage: www.elsevier.com/locate/matdes

Short Communication

Mechanical alloying behavior of Ti6Al4V residual scraps with addition of Al_2O_3 to produce nanostructured powder

A. Mahboubi Soufiani *, M.H. Enayati, F. Karimzadeh

Department of Materials Engineering, Isfahan University of Technology, Isfahan 84156-83111, Iran

ARTICLE INFO

Article history:
Received 5 January 2010
Accepted 20 March 2010
Available online 27 March 2010

ABSTRACT

The present investigation has been based on production and subsequent comparison of different physical, mechanical and thermal properties of nanostructured Ti6Al4V and Ti6Al4V/Al_2O_3 powders by means of high energy ball milling. In this regard, the structural and morphological changes of powders were investigated by X-ray diffraction, scanning electron microscopy and microhardness measurements. The results revealed that ball milling process reduced the grain size of Ti6Al4V and Ti6Al4V + 10 wt% Al_2O_3 to approximately 20 and 15 nm, respectively. For both compositions also a remarkable change in morphology and particle size occurred during ball milling of powders with different compositions. Moreover, phase evolution during milling and heat treatment was taken into consideration. The as-milled Ti6Al4V + 10 wt% Al_2O_3 powder exhibited higher microhardness (~900 Hv) comparing to as-milled Ti6Al4V (~536 Hv) and as-received samples (~400 Hv).

1. Introduction

Titanium and titanium alloys have been widely employed in industrial and biomedical applications because of relatively low module of elasticity, low-density, high specific strength, good biocompatibility and corrosion resistance [1–3]. On the other hand these appealing characteristics are accompanied by relatively poor tribological properties and low hardness [4].

Metal matrix composites (MMCs) have provided increased mechanical and physical properties at usually less weight than unreinforced metallic materials because of the addition of low-density, high modulus reinforcements which compensate the matrix's shortcomings [5]. Among this, titanium matrix composites (TMCs) have attracted much attention due to the good combination of low-density and excellent mechanical properties at service temperature [6]. Ti6Al4V as an $\alpha + \beta$ titanium alloy, has proven to be the most promising titanium alloy especially for aerospace, medical and marine applications. In the last couple of decades, extensive and intensive investigations have been done on production of particle reinforced titanium and titanium alloys by cold and hot pressing, combustion assisted synthesis, self-propagation high temperature synthesis and solidification processes [7]. In this regards the effects of addition of TiC, SiC and TiB/TiB_2 particles to titanium matrix has been studied [8–10]. However, there are only few reports dealing with fabrication of titanium alloy based micro and nanocomposite by powder metallurgy [11–13].

In the recent years, nanostructured materials have gained considerable attention due to their improved properties in comparison with micro sized structure materials [14]. In this regard, a wide range of investigations have been devoted to the alternations in mechanical, thermal, magnetic and diffusion characteristics of nanocrystalline materials [15,16].

Most production processes, such as machining and forging, leave over scraps of titanium alloys [17]. These scraps, approximately, hold 40% of initial raw materials used in manufacturing of different parts with various sizes, in terms of waste [18]. Moreover, considering the enormous amount of titanium and its alloys used in different sections of industry, it is of a great economic, strategic and environmental importance to find proper methods in order to recycle and reuse the manufacturing scraps [19]. Previously researchers have studied producing titanium and aluminum powders from residual chips by severe plastic deformation methods [20–23].

One of the most cost effective methods that has been proven to be able of producing powders with nano sized structure is mechanical alloying (MA) [24]. This process has been utilized in fabrication of different products such as nanostructured intermetallic compounds and metal matrix composites [25–27].

The current study, therefore, is set up to aim at producing nanostructured Ti6Al4V based composite by means of mechanical alloying (MA) from industrial residual scraps. The present report focused mainly on the characterization and simultaneously, some preliminary measurements on the thermal, mechanical and physical properties of the nanostructured Ti6Al4V and Ti6Al4V + 10 wt% Al_2O_3 powders.

* Corresponding author. Tel.: +98 9133142314; fax: +98 3113912751.
E-mail address: a.soofiani@ma.iut.ac.ir (A. Mahboubi Soufiani).

0261-3069/$ - see front matter © 2010 Elsevier Ltd. All rights reserved.
doi:10.1016/j.matdes.2010.03.037

2. Experimental procedure

The scraps used in this investigation were residual machining chips of Ti6Al4V bars. The composition of the as-received chips was determined using quantometer analysis (Table 1). The machining chips had a spring-like morphology, in order to reduce the size of chips, first they were crushed in a mortar to obtain fine chips suitable for ball milling (Fig. 1a and b). The optical microscopic image of the macro etched sample shows grains of about 46 μm (Fig. 1c), whilst the SEM micrograph of the micro etched sample presents the $\alpha + \beta$ structure of Ti6Al4V chips with α being the dark background and β the bright zones (Fig. 1d). Al_2O_3 nanoparticles were used as reinforcement in order to produce Ti6Al4V + 10 wt% Al_2O_3 nanocomposite (Fig. 1e).

Mechanical milling was applied under protective atmosphere of Ar (99.998% pure) in a planetary ball mill. Milling parameters are given in Table 2.

Sampling was done from milled materials after different time periods. Powder samples were subjected to heat treatment in a tube furnace under an Ar atmosphere at 600 °C for 1 h. The structure and phase composition of mechanically milled and heat treated powders were characterized by means of X-ray diffraction (Philips X'PERT MPD) using filtered Cu Kα radiation (λ = 0.1542 nm). The morphologies and particle size of milled powders were determined utilizing scanning electron microscope (Philips XL30), and optical microscope (OP).

Table 2
Milling parameters.

Ball mill machine	Planetary
Rotation speed of vial (rpm)	500
Vial material	Hardened Cr steel
Vial capacity (ml)	120
Ball material	Hardened carbon steel
Diameter of balls (mm)	20
Number of balls	5
Ball to powder weight ratio	10:1
Total powder mass (g)	16.3

The average crystallite size and internal strain in the milled samples were calculated from the XRD peak broadening using the Williamson–Hall equation (1) [28]:

$$\beta \cos\theta = \frac{k\lambda}{D} + 2A\sqrt{(\varepsilon)^2}\sin\theta \quad (1)$$

where θ is the Bragg diffraction angle, D the average crystallite size, ε the average internal strain, λ the wave length of the radiation used (0.15406 nm), β the diffraction peak width at half maximum intensity, K the Scherrer constant (0.9) and A is the coefficient which depends on the distribution of strain; it is near to unity for dislocations. In the Williamson–Hall method, both of broadening contributions, due to the strain and crystalline size, are taken into account.

Table 1
Chemical composition of as-received chips.

Element	Ti	Al	V	Cu	Mo	Sn	Nb	Fe	Pd	Zr	Mn
Concentration (wt%)	87.85	6.09	3.12	<1.0	<0.5	<0.5	<0.5	0.311	0.184	<0.1	<0.1

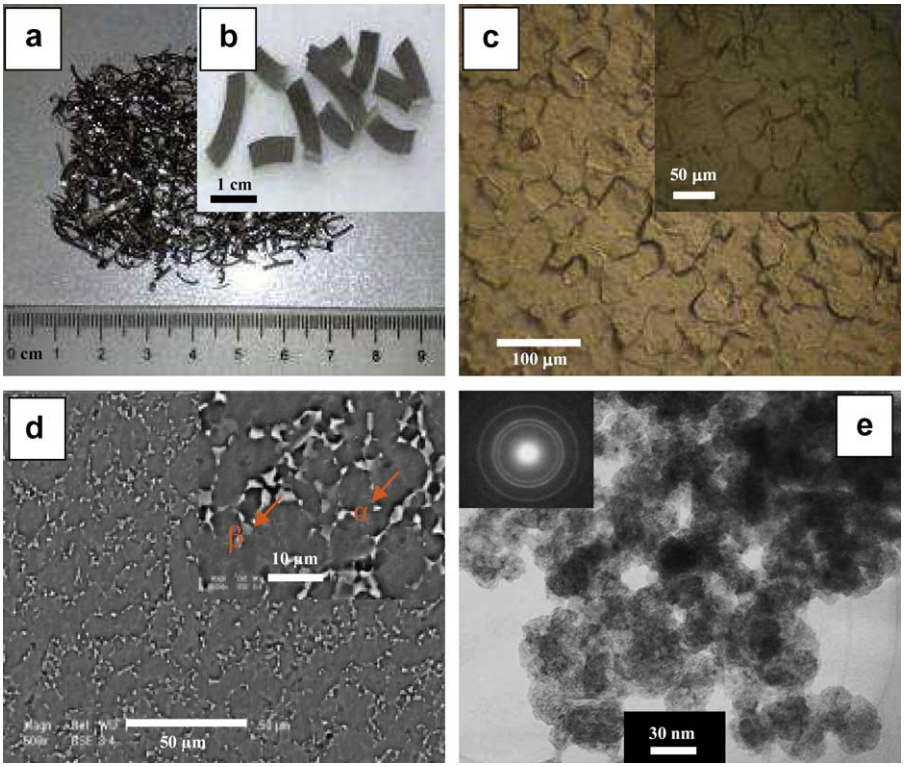

Fig. 1. (a) As-received Ti6Al4V chips (b) hand-blended chips (c) the microstructure of the macro etched (H_2O 96%, HNO_3 2.5%, HF 1.5%) chips under optical microscope (d) SEM micrograph of the microstructure of the micro etched (H_2O 80%, HNO_3 2%, HF 6%) chips (e) TEM image of Al_2O_3 nanoparticles.

Microhardness test was carried out at the load of 37.64 g and the dwell time of 5 s. Five indentations were made on each sample to obtain an average value of microhardness. The microhardness measurement was carried out on the cross-section of powder particles. The samples were prepared by mounting a small amount of powder in a carbon-base conductive resin followed by conventional grinding and polishing methods.

3. Results and discussion

3.1. Morphological analysis

In order to study the microstructural and morphological changes of samples during ball milling, a small amount of powder were taken after 5, 10, 20, 30, 40 and 50 h of milling time for SEM

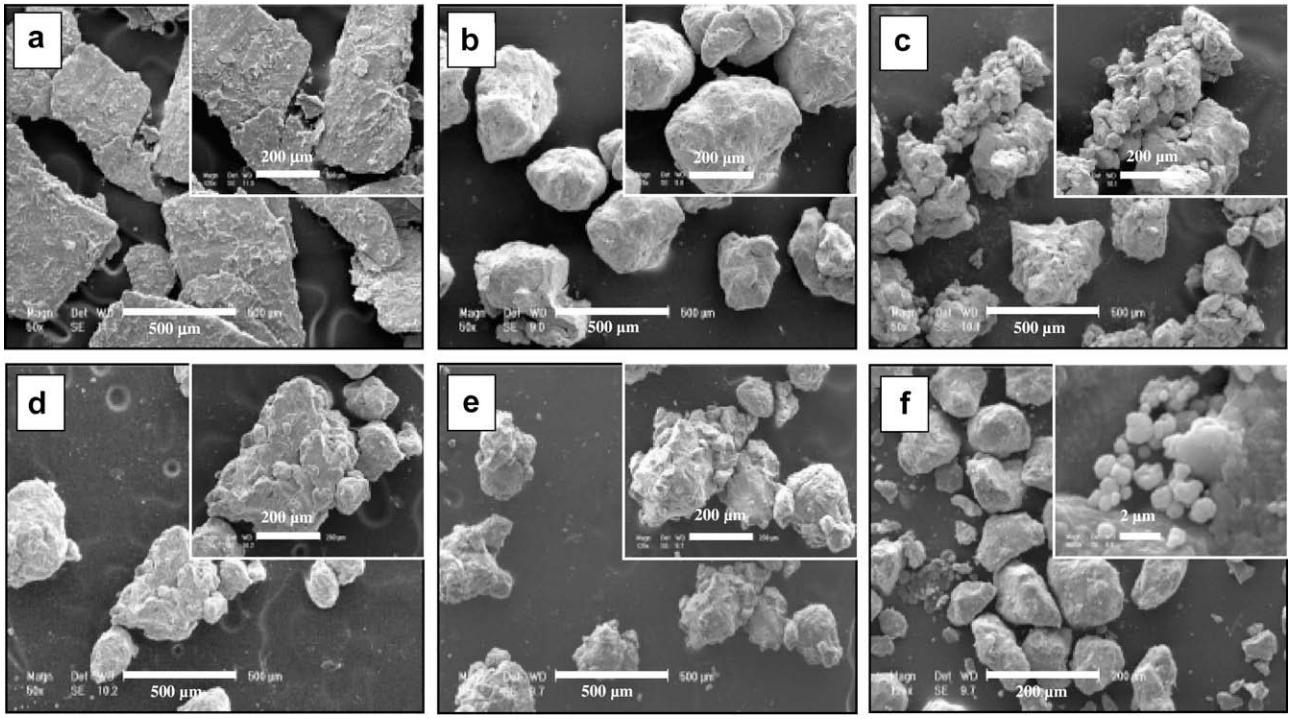

Fig. 2. SEM micrographs of Ti6Al4V powders milled in planetary ball mill for (a) 5 h (b) 10 h (c) 20 h (d) 30 h (e) 40 h (f) 50 h (Images with higher magnification are presented in insets).

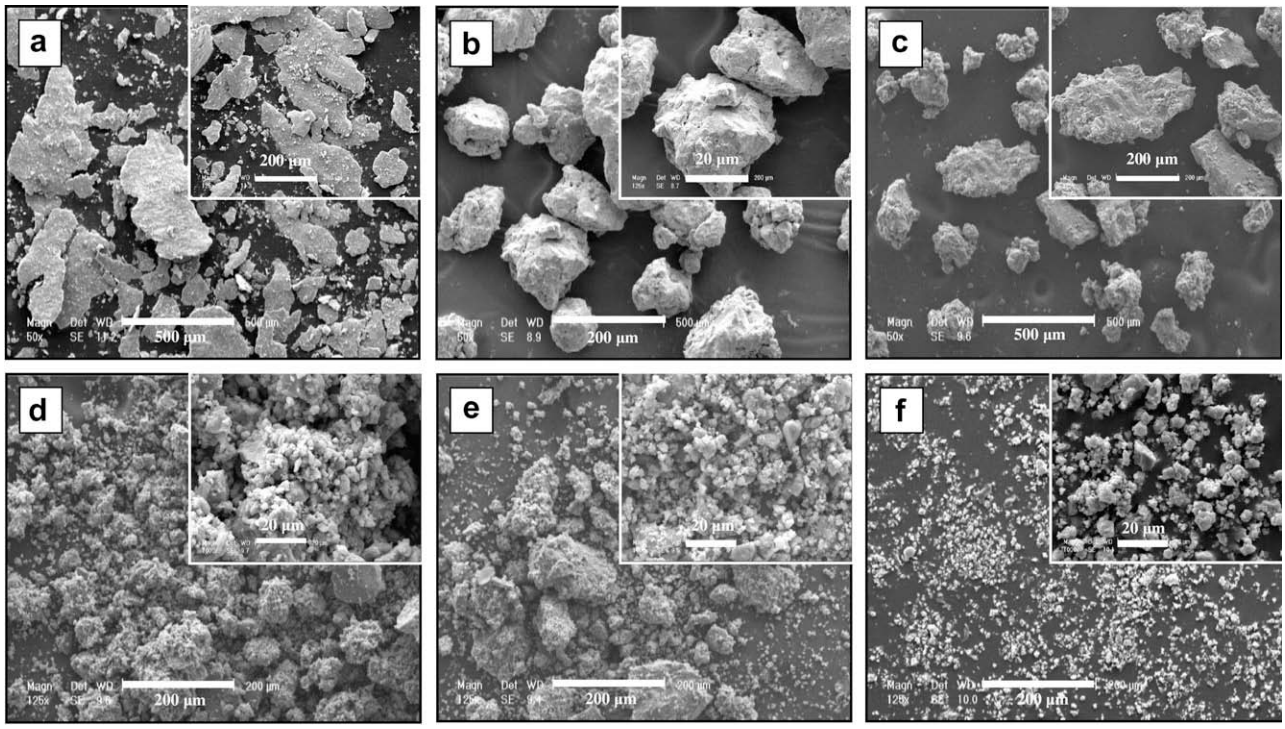

Fig. 3. SEM micrographs of Ti6Al4V + 10 wt% Al_2O_3 powders milled in planetary ball mill for (a) 2 h (b) 10 h (c) 20 h (d) 30 h (e) 40 h (f) 50 h.

observations (Fig. 2). As Fig. 2a indicates, after 5 h of milling powder particles have still preserved their flake like shape. With increasing milling time, due to the gradually repeated cold welding, fracturing, and severe plastic deformation the powder particles become equiaxed in shape (Fig. 2b). Although with continuing milling up to 20 h the powder particles size follows a decreasing trend. At this stage fine powder particles start to agglomerate and from large cluster (Fig. 2c). With increasing milling time to 30 and then 40 h (Fig. 2d, e), the clusters become smaller in size so that eventually after 50 h there are clusters of 80 μm diameter consisting of ~1 μm particles. The plot in Fig. 4a illustrates the changes in powder particle size with milling time.

To evaluate the effects of Al_2O_3 addition, Ti6Al4V chips were also ball milled with 10 wt% Al_2O_3 nanopowder under identical conditions. As it can be seen in Fig. 3, a particle size reduction trend is dominant. After 2 h of milling flake-like particles still exist, while by increasing milling time to 10 h, the particles become equiaxed in shape (Fig. 3a and b). With approaching to 20 h of milling time these equiaxed particles are crushed into smaller particles (Fig. 3c). From 20 to 30 h of milling time the powder particle size decreases dramatically from ~225 μm to ~6 μm. At this stage agglomerated clusters consist of very fine particles (Fig. 3d). Comparing the 40 h milled powders of Ti6Al4V + Al_2O_3 and Ti6Al4V there seems to be a great difference, where the composite powder particles (~2 μm) are significantly smaller (Fig. 3e). This behavior reflects the role of Al_2O_3 nanoparticles added to the scrap which diminishes the cold welding process and moreover, increases work hardening by creating dislocation forests followed by intense dislocation pile-ups [29,30]. This therefore leads to the enhancement of brittleness and fracturing of powder particles during mechanical milling as has been reported in previous investigations [31,32]. Moreover, final powder particles produced after 50 h of milling are generally fine (~4 μm) and dispersed (Fig. 3f).

The plot in Fig. 4 illustrates the changes in particle size with milling time for both Ti6Al4V and Ti6Al4V + 10 wt% Al_2O_3 powders. The graphs show that particle size of Ti6Al4V scraps reduces gradually with milling time while it sharply declines after 10 h of milling for the composite sample. The sharp reduction of powder particle size in presence of Al_2O_3 particles has also been observed by Prabhu et al. [32]. As it was expected, samples containing Al_2O_3 particle gain their final size in shorter milling times (30 h of milling time) and also the resulting powder particles are much finer (Fig. 4b), than that in case of Ti6Al4V (Fig. 4a).

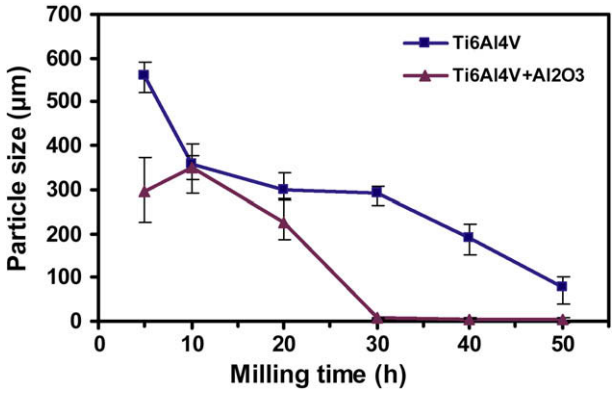

Fig. 4. Changes in powder particle size with milling time for Ti6Al4V and Ti6Al4V + 10 wt% Al_2O_3.

3.2. Phase evaluation during milling

Fig. 5 indicates the XRD patterns of Ti6Al4V as-received and after 20 and 40 h of ball milling. As it can be seen after 20 h of milling the intensity of the main peaks have gradually reduced and peak broadening has occurred. With further milling up to 40 h, excessive peak broadening takes place and the sharpness of $\beta(1\,1\,0)$, $\alpha(1\,0\,1)$ peaks and the intensity ratio of $\alpha(1\,0\,3)/\beta(2\,1\,1)$ greatly declined. This phenomenon is a sign of Ti6Al4V alloy grain size reduction down to nanometer scale [28].

The XRD patterns of Ti6Al4V scraps containing 10 wt% Al_2O_3 milled for 2, 10, 20 and 40 h is represented in Fig. 6. A dramatic decrease in the intensity of $\beta(1\,1\,0)$, $\alpha(1\,0\,1)$ peaks and $\alpha(1\,0\,3)/\beta(2\,1\,1)$ intensity ratio can be seen after 10 h of milling time. With milling of the composite powder up to 20 h, crystallite size of about 15 nm is achieved and the structure starts to transform to an amorphous state. It is worth to note that the XRD pattern of 10 h milled Ti6Al4V + Al_2O_3 is similar to that for Ti6Al4V powder after 20 h of milling time. This reveals the effectiveness of added nanoparticles in accelerating grain size reduction [33]. This enhanced grain size reduction in powder samples with Al_2O_3 is related to the effect of these nanoparticles on elevating dislocation density [33]. After 40 h of milling, as is featured in Fig. 6, a partially amorphous structure has been achieved. It should be noted that, because of the small fraction (10 wt%) of Al_2O_3 along with its nano-sized particles, the XRD peaks of Al_2O_3 are very broaden with low intensity [32]. As a result Al_2O_3 peaks become invisible on XRD patterns. This phenomenon was observed in previous studies [34,35].

The crystallite size and internal strain of samples after different milling times were measured by Williamson–Hall method and reported in Table 3. As it can be seen the value of internal strain is significantly greater for the Ti6Al4V + Al_2O_3 powder samples, which is due to the effect of added Al_2O_3 nanoparticles on elevating lattice strain. The presence of hard second phase particles changes

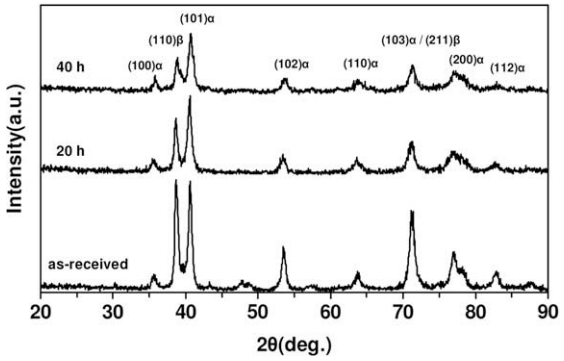

Fig. 5. XRD patterns of Ti6Al4V samples as-received and after 20 and 40 h ball milling.

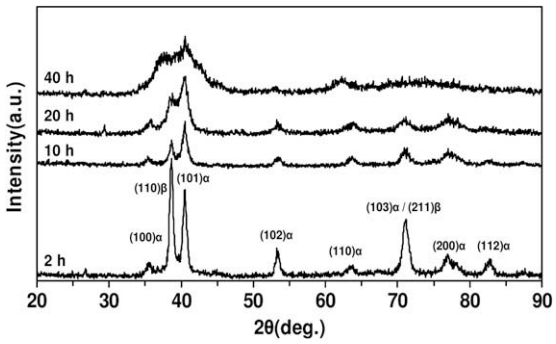

Fig. 6. XRD patterns of Ti6Al4V + 10 wt% Al_2O_3 samples after 2, 10, 20 and 40 h ball milling.

Table 3
The crystallite size and internal strain of Ti6Al4V and Ti6Al4V + 10 wt% Al_2O_3 powders.

Milling time (h)	Crystallite size (nm)	Internal strain (%)
20 (Ti6Al4V)	95	0.43
40 (Ti6Al4V)	20	1.4
10 (Ti6Al4V + 10 wt% Al_2O_3)	80	2.4
20 (Ti6Al4V + 10 wt% Al_2O_3)	15	3.1

the local dislocation density distribution, due to strain incompatibility between the matrix and particles which may cause excessive accumulation of internal strain [36,37].

3.3. Thermal behavior

Fig. 7 represents XRD patterns of as-milled and heat treated Ti6Al4V and Ti6Al4V + 10 wt% Al_2O_3 powders. The two samples have been through the same cycle of milling and heat treating (40 h milling + 1 h isothermal heating at 600 °C). The 40 h ball milled Ti6Al4V powder possesses a nanosized structure (~20 nm). After annealing all main Ti6Al4V peaks have sharpened and intensified. These changes obviously present enormous unwanted grain growth.

On the other hand, as shown in Fig. 8 that the Ti6Al4V powder containing 10 wt% Al_2O_3 has an amorphous structure after 40 h of milling. This different behavior that result from the addition of Al_2O_3 may be due to the role of Al_2O_3 in dislocation and grain boundary pinning [38].

In contrast to Ti6Al4V powders, there seems to be no significant changes in the microstructure of the 40 h milled Ti6Al4V + 10 wt% Al_2O_3 powder sample after annealing, except the sharpening of the

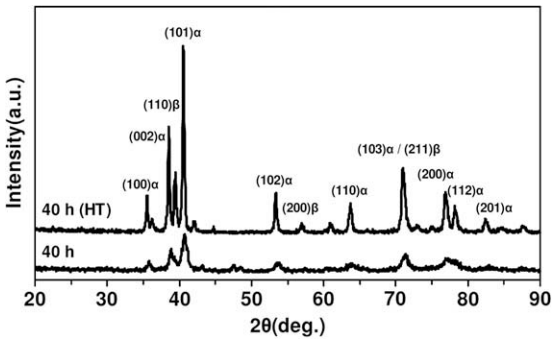

Fig. 7. XRD patterns of Ti6Al4V sample as-milled for 40 h and after subsequent annealing for 1 h at 600 °C.

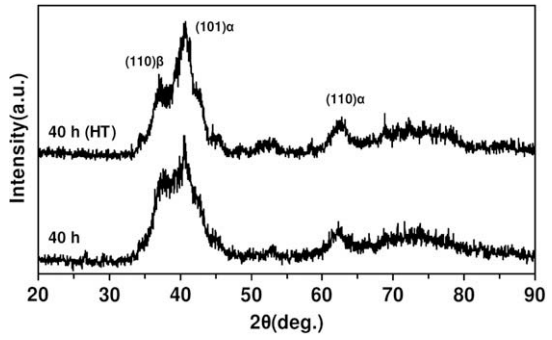

Fig. 8. XRD patterns of Ti6Al4V + 10 wt% Al_2O_3 powder as-milled for 40 h and after subsequent annealing for 1 h at 600 °C.

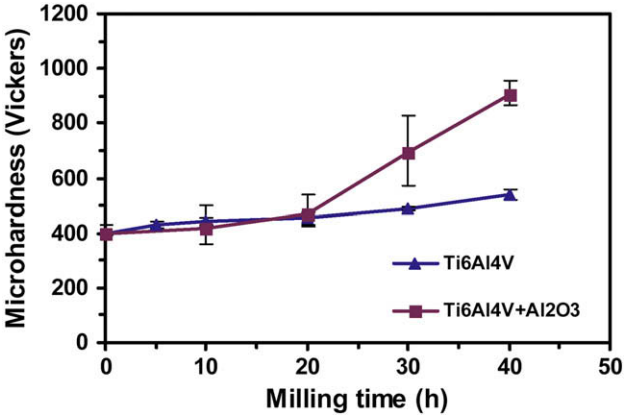

Fig. 9. Variation of microhardness value with milling time for Ti6Al4V and Ti6Al4V + 10 wt% Al_2O_3 powders.

main peak of α(1 0 1). This result suggests that the amorphous phase produced by ball milling of Ti6Al4V + Al_2O_3 composition is stable against crystallization.

3.4. Microhardness measurements

The results of microhardness measurements of Ti6Al4V and Ti6Al4V + 10 wt% Al_2O_3 powder samples milled for various time periods are shown in Fig. 9. After 40 h of ball milling the hardness of Ti6Al4V powder reaches to 536 Hv, whilst it was 400 Hv for the as-received scraps (Fig. 9a). On the other hand, the hardness of Ti6Al4V + Al_2O_3 powder had a sharp incline after 20 h of milling that is due to formation of hard amorphous phase, in agreement with XRD results (Fig. 6). From 20 to 40 h hardness value increases to 900 Hv (Fig. 9b). This significant difference between hardness of Ti6Al4V and Ti6Al4V + Al_2O_3 composite powder may be due to the strong effect of Al_2O_3 nanoparticles on enhancement of work hardening [33].

4. Conclusions

The main objective of this work was to study the mechanical alloying behavior of Ti6Al4V residual scraps to produce nanostructured powder:

(1) The effect of Al_2O_3 nanoparticles on powder particle size reduction was significant. The Ti6Al4V powder containing 10 wt% Al_2O_3 reached a particle size of ~4 μm after 30 h, while Ti6Al4V powder attained a particle size of ~80 μm after 50 h of ball milling.
(2) The Al_2O_3 nanoparticles dispersed in Ti6Al4V matrix accelerated the trend of grain size reduction by fixing dislocations and helping dislocation pile ups and enhancing the internal strain, which result in production of more high-angle grain boundaries and finally finer grains. After 20 of milling the crystallite size of the Ti6Al4V + Al_2O_3 composite powder was measured to be about 15 nm, where it was 90 nm for the Ti6Al4V powder.
(3) Ti6Al4V powders showed significant grain coarsening after annealing for 1 h in 600 °C, however, the Ti6Al4V + Al_2O_3 composite powder with a partially amorphous structure was remained untouched.
(4) Microhardness measurements showed a dramatic difference between the hardness of Ti6Al4V powder (~536 Hv) and the Ti6Al4V + Al_2O_3 composite (~900 Hv). This difference variation reveals the influence of Al_2O_3 on enhancement of work hardening and subsequent amorphization.

References

[1] Ggonzalez JEG, Mirza-Rosca JC. Study of the corrosion behavior of titanium and some of its alloys for biomedical and dental implant applications. J Electroanal Chem 1999;471:109–15.
[2] Mu Y, Kobayashi T, Sumtta M, Yamamoto A, Hanawa T. Metal ion release from titanium with active oxygen species generated by rat macrophages in vitro. J Biomem Mater Res 2000;49:283–7.
[3] Browne M, Gregson PJ. Effect of mechanical surface pretreatment on metal ion release. Biomaterials 2000;21:385–92.
[4] Liu X, Chu PK, Ding CH. Mater Sci Eng R 2004;47:49–56.
[5] Karl U. Metal matrix composites-custom-made materials for automotive and aerospace engineering. Weinheim: Wiley-VCH Verlag; 2006.
[6] Niespodziana K, Jurczyk K, Jurczyk M. Titanium-ceramic nanocomposites fabricated by the mechanical alloying process. Mater Sci Poland 2008;26:341–8.
[7] Kim MG, Sung SY, Kim YJ. Synthesis of in-situ titanium carbide particle reinforced titanium composites. Mater Sci Forum 2005;475–479:963–6.
[8] Ranganath S, Roy T, Mishra RS. Microstructure and deformation of TiB+Ti2O reinforced titanium matrix composites. Mater Sci Tech 1996;12:219–25.
[9] Soboyejo WO, Lederich RJ, Sastry SML. Mechanical behavior of damage tolerant TiB wisker-reinforced in situ titanium matrix composites. Acta Metall Mater 1994;42:2579–91.
[10] Tjong SC, Ma ZY. Microstructural and mechanical characteristics of in situ metal matrix composites. Mater Sci Eng R 2000;29:49–113.
[11] Popa C, Simon V, Vida-simiti I, Batin G, Candea V, Simon S. Titanium–hydroxyapatite porous structures for endosseous applications. J Mater Sci Mater Med 2005;16:1165–71.
[12] Chenglin C, Jingchuan Z, Zhongda Y, Shidong W. Hydroxyapatite–Ti functionally graded biomaterial fabricated by powder metallurgy. Mater Sci Eng A 1999;271:95–100.
[13] Ning CQ, Zhou Y. In vitro bioactivity of a biocomposite fabricated from HA and Ti powders by powder metallurgy method. Biomaterials 2002;23:2909–15.
[14] Morris DG. Mechanical behavior of nanostructured materials. Trans Tech Publications 1998.
[15] Zhu KY, Vassel A, Brisset F, Lu K, Lu J. Nanostructure formation mechanism of a-titanium using SMAT. Acta Mater 2004;52:4101–10.
[16] Lauer S, Guan Z, Wolf H, Wichert Th. Structural investigations of nanocrystalline Ti–Al and Ni by PAC. Hyperfine Interact 1999;120/121:307–12.
[17] El-Morsy A. Microstructural characterization of Ti–6Al–4V machining chips after remelting and severe deformation. Mater Des 2009;30:1825–9.
[18] Gambogi J. Recycling-metals. US geological survey minerals yearbook; 2000.
[19] Ishi M, Kinoshita K. Titanium products as environmental friendly materials. Nippon steel technical report; 2000.
[20] Forouzanmehr N, Enayati MH, Karimzadeh F. Fabrication and characterization of nanostructure Ti powder from residual machining chips. In: First international congress on nanoscience and nanotechnology December 2006.
[21] Razavi M, Rahimpour MR, Rajabi-Zamani AH. Synthesis of nanocrystalline TiC powder from impure Ti chips via mechanical alloying. J Alloys Compd 2007;436:142–5.
[22] Samoshina M, Aksenov A, Kaevitser E. Structure and properties of mechanically alloyed composite materials from hard-recycling scrap of Al alloys. Rev adv Mater Sci 2008;18:305–11.
[23] Hong S, Lee D, Kim B. Manufacturing of aluminum flake powder from foil scarp by dry ball milling process. J Mater Process Technol 2000;100:105–9.
[24] Suryanarayana C. Mechanical alloying and milling. Prog Mater Sci 2001;46:1–184.
[25] Zakeri M, Yazdani-Rad R, Enayati MH, Rahimipour MR. Preparation of Al_2O_3–TiC nanocomposite by mechano-chemical reduction of TiO_2 with aluminum and graphite. J Alloys Compd 2009;481:320–5.
[26] Hwang SJ, Lee J. Effect of ternary addition on mechanical properties of TiAl. Acta Mater 1998;46:2185–94.
[27] Rafie M, Enayati MH, Karimzadeh F. Characterization and formation mechanism of nanocrystalline (Fe, Ti) 3Al intermetallic compound prepared by mechanical alloying. J Alloys Compd 2009;480:392–6.
[28] Williamson GK, Hall WH. X-ray line broadening from field aluminum and wolfram. Acta Metal 1953;1:22–31.
[29] Clyne TW, Withers PJ. An introduction to metal matrix composites. Cambridge: Cambridge University Press; 1992.
[30] Lewandowski JJ, Liu C, Hunt WH. Effects of matrix microstructure and particle distribution on fracture of an aluminum metal matrix composite. Mater Sci Eng 1989;107:241–55.
[31] Ling Z, Luo L, Dodd B. Experimental study on the formation of shear bands and effect of microstructure in AI-2124/SiCp composites under dynamic compression. J Phys III 1994;4:453–8.
[32] Prabhu B, Suryanarayana C, Vaidyanathan R. Synthesis and characterization of high volume fraction Al–Al_2O_3 nanocomposite powders by high-energy milling. Mater Sci Eng A 2006;425:192–200.
[33] Ahmed A, Neely AJ, Shankar K. Effect of ceramic reinforcements on the mechanical behavior of 7xxx series aluminum matrix composites. In: 5th Australasian congress on applied mechanics, Brisbane, Australia; 2007..
[34] Wu JM. Nano-sized amorphous alumina particles obtained by ball milling ZnO and Al powder mixture. Mater Lett 2001;48:324–30.
[35] Tavoosi M, Karimzadeh F, Enayati MH. Fabrication of Al–Zn/α-Al_2O_3 nanocomposite by mechanical alloying. Mater Lett 2008;62:282–5.
[36] Cottrell AH. Theoretical structural metallurgy. J Geol 1950;58:90.
[37] Apps P, Prangnell PB. Grain refinement mechanisms operating during severe plastic deformation of aluminum alloys containing second phase particles. In: Zhu YT, editor. Ultrafine grained materials-III. Pennsylvania: TMS; 2004. p. 131–6.
[38] Bachmaier A, Hohenwarter A, Pippan R. New procedure to generate stable nanocrystallites by severe plastic deformation. Scripta Mater 2009;61:536–9.